Damages on complex structural systems: Effects on load paths

International Journal of Solids and Structures 311 (2025) 113213

Contents lists available at ScienceDirect

International Journal of Solids and Structures

journal homepage: www.elsevier.com/locate/ijsolstr

Damages on complex structural systems: Effects on load paths

Lorenza Abbracciavento, Valerio De Biagi *

Dept. of Structural, Geotechnical and Building Eng., Politecnico di Torino, Corso Duca degli Abruzzi 24, Torino, 10129, Italy

ARTICLE INFO

Keywords:
Structural complexity
Load path
Redundancy
Robustness

ABSTRACT

In the event of damage to a structural system, ensuring the redistribution of loads becomes crucial to mitigate the risk of progressive collapse. By providing alternative load paths, structures can accommodate load redistribution, adapting to progressive changes in structural conditions over time, reducing the probability of failure and demonstrating increased robustness. In conventional redundant structures, say frames, the main behavior is expected to be parallel-like, with individual load paths within the structure capable of interacting and redistributing loads in response to localized changes. The alteration of the stiffness of one element due to damage may cause a change of the overall behavior. In this paper it is shown that the evolution of a random damage on the structure, in particular when the arrangement of the element is non-trivial, highlights a transition between the overall behavior of the system. Specifically, as damage progresses, the system may shift from parallel-like to series-like, typical in non-redundant structures, with consequent dramatic and potentially non-robust situations. Examples on simple structures are provided to highlight the difference in the behaviors.

1. Introduction

Systems working in *series* and in *parallel* are commonly used in many disciplines and application areas for analysis and design purposes (Tavakkoli-Moghaddam et al., 2008). The theories of series and parallel systems find extensive practical application in technical and nontechnical fields, serving as key components for enhancing efficiency and resilience. In electrical power systems, parallel configurations ensure continuity of service by providing alternative pathways for electricity, thereby mitigating the impact of failures in single components (Ouiddir et al., 2004). Similarly, transportation systems leverage parallel routing to optimize traffic flow and reduce congestion, enhancing throughput and system responsiveness (Levitin and Lisnianski, 2001; Hagen and Tvedt, 1991). In telecommunications, redundancy provided by parallel pathways is crucial for maintaining uninterrupted communication in the event of network failures or overloads (Khabbaz et al., 2011; Lyu et al., 2002). Beyond these applications, parallel and series systems play vital roles in hydraulic engineering, contributing to efficient water distribution and flood management (Roberson et al., 1998). Similarly, computing networks rely on redundant data pathways to enhance reliability and speed, which is crucial for maintaining data integrity in high-performance environments (Chen et al., 1994; Zissis and Lekkas, 2012; Song and Der Kiureghian, 2003; Mahmood et al., 2015). Moreover, the principles of serial and parallel configurations are instrumental in safety-critical systems in aerospace engineering, where system redundancy can be a matter of life and death (Pathan, 2017; Chen, 2018). The principles of these configurations extend into cybersecurity, where multiple layers of security controls (defense in depth) are employed to protect data and prevent unauthorized access (Mughal, 2018). Network engineering utilizes parallel pathways to ensure consistent and reliable data transmission, critical in maintaining high availability and performance across global networks (Akyildiz et al., 2014; Sterbenz et al., 2010). Beyond technology, in biomedical engineering, parallel processing techniques in imaging systems like MRI and CT scans enhance the speed and accuracy of diagnostic processes (Saxena et al., 2013) finding wide implementation also in the field of materials engineering (Nelson and Dorfmann, 1995; Bažant et al., 2004; Bazant and Prasannan, 1989; Bažant et al., 1996). The concepts are also pivotal in manufacturing systems where parallel assembly lines increase production rates and flexibility, allowing for more robust responses to demand fluctuations and operational disruptions (Majdzik, 2022). In environmental engineering, series and parallel treatments in water purification systems enable more effective and resilient management of water resources (Pillai, 2024).

Despite the extensive use of series and parallel configurations across various engineering disciplines, their integration into civil structural engineering, specifically regarding a formalized framework for load transfer metrics and robust design methodologies, remains limited. This gap is particularly significant in understanding progressive structural collapse and during the design phase aimed at creating more robust structures. However, in this regard, substantial contributions have been

* Corresponding author.
E-mail address: valerio.debiagi@polito.it (V. De Biagi).

https://doi.org/10.1016/j.ijsolstr.2024.113213
Received 9 October 2024; Received in revised form 14 November 2024; Accepted 30 December 2024
Available online 22 January 2025

made in the field of design-for-reliability studies (Hohenbichler and Rackwitz, 1983; Yalaoui et al., 2005; Bier et al., 2005; Coit and Smith, 1996). Reliability engineering, a sub-discipline of systems engineering, focuses on enhancing the capability of systems to operate without failures (Zio, 2009). In civil engineering, this translates into strategies for allocating redundancies effectively, a principle deeply explored under the 'design-for-reliability' banner. Such strategies include the deployment of alternative load paths, where redundancy in structural elements allows for multiple pathways for load distribution, essential for maintaining structural integrity when certain pathways are compromised (Starossek and Haberland, 2011; Starossek, 2009; Kiakojouri et al., 2020). Although the 'design for robustness' (Taflanidis et al., 2008; Knoll and Vogel, 2009; De Biagi and Chiaia, 2013; Kiakojouri et al., 2023) has been addressed in existing literature, it lacks comprehensive models that effectively consolidate the understanding of load transmission behaviors in both series and parallel configurations within structural systems.

This study introduces a novel model that, first, addresses this gap and, second, investigates the impact of element damage within the system. Thanks to a specific metric, it analyzes how the load path is altered and redistributed within the structure following damage. The analysis of a mechanical system made by rods working in series and parallel is herein proposed. The purpose of this study is to analyze the effects of the propagation of damage within a series and parallel system and investigate how the redistribution of load paths varies as the evolution of damage propagation advances. The study is expanded to more articulated systems, like a small truss structure, to highlight the capabilities of the proposed metrics.

2. Problem statement

De Biagi and Chiaia (2016) have studied the behavior of parallel systems, demonstrating that such systems offer an optimal structural robustness in all situations where load paths are equally distributed among all elements. When removing a random element from a system operating in parallel, the remaining elements compensate for its absence in the most optimal efficient manner. This phenomenon can be attributed to the fact that, the contribution of each element is equal to that of every other element within the system, ensuring that all operate perfectly in parallel. This scenario is characterized by equally important load paths for all elements, a condition achieved when the stiffnesses are equal.

This concept finds its extreme opposite in series systems, where the removal of one element leads to the complete crisis of the system. Nonetheless, intermediate scenarios, which more accurately reflect real-world conditions by incorporating both serial and parallel components, constitute a largely unexplored domain. The present study addresses this inadequately investigated area.

Two conceptual examples illustrating how the concept of mixed series–parallel systems can be recognized and implemented in real-world structures are presented below.

Example 1. Consider the image in Fig. 1, showing the components of the pier structural element. The foundation piles of Fig. 1.(b) are characterized, each, by a stiffness $k_{p,i}$ and they form a system working in parallel expressed in Eq. (1) since the total stiffness of the foundation is given by the sum of the stiffnesses of the individual foundation piles:

$$K_f = k_{p,1} + k_{p,2} + k_{p,3} + k_{p,4}. \tag{1}$$

Similarly, the bearing system of Fig. 1.(a) also represents a system working in parallel since the total stiffness is given by the sum of the stiffnesses of the individual bearing devices $k_{b,i}$:

$$K_b = k_{b,1} + k_{b,2} + k_{b,3}. \tag{2}$$

Consider instead the image in Fig. 1.(c), where the analysis shifts from the scale of the components to the scale of the structural element. The total stiffness of the pier may be described as the result of a system working in series, i.e., foundation, shaft and bearing support system in Fig. 1.(d), and therefore it will be given by:

$$\frac{1}{K_{PIER}} = \frac{1}{K_f} + \frac{1}{K_s} + \frac{1}{K_b}. \tag{3}$$

Consequently, the total description of bridge substructure (Fig. 2) is straightforward as:

$$K_{eq,substruct} = K_{PIER,1} + K_{PIER,2} + K_{PIER,3}. \tag{4}$$

To fully grasp the power of this concept, it is essential to explore how it applies in a specific scenario. Therefore, consider the horizontal braking force F with action vector parallel to the longitudinal axis of the bridge. The displacement δ at the head of the pier will be the same for each pier, assuming the deck is infinitely rigid. The total displacement δ expressed in Eq. (5) is the sum of three contributions: the displacement due to the deformability of the foundations system δ_f, the displacement due to the deformability of the shaft δ_s and the displacement due to the deformability of the bearing support system δ_b as depicted in Fig. 2 (Manterola, 2015).

Assuming that everything takes place in the linear elastic field, the total displacement can be thus calculated as follow:

$$\begin{aligned}\delta &= \delta_f + \delta_s + \delta_b \\ &= \frac{F}{K_f} + \frac{F}{K_s} + \frac{F}{K_b} = \frac{F}{K_{PIER}},\end{aligned} \tag{5}$$

hence, the total stiffness of the pier K_{PIER} is detailed in Eq. (3).

Example 2. The structure shown in Fig. 3.(a) is a shear-type frame subjected to horizontal loading F. In accordance with the central concept, the structure can be simplified into a diagram of elements arranged in a non-trivial manner. Under the hypothesis of infinitely rigid floors (Chopra, 2007; Prasad, 2020), the structure can be simplified to the diagram depicted in Fig. 3.(b). However, under the hypothesis that the vertical elements are far more rigid that the horizontal ones, the simplification of the system changes, see Fig. 3.(c). While this may seem like a minor modification, it leads to two distinctly different patterns of load redistribution (Weng et al., 2020).

The main idea in this paper is to develop these concepts extending the approach proposed by De Biagi and Chiaia (2016) on systems in parallel to those in series and to systems with rods arranged in a non-trivial manner. This method aims at simplifying the overall behavior of structural systems into reduced diagrams representing the elements and their mechanical properties, creating a unified theory capable of comprehensively describing the global behaviors and the interaction between elements.

3. Methodology

The proposed methodology entails simplifying complex structural systems into structural schemes by representing them with rod-based configurations. The mechanical characteristics of the rods are defined by their elasticity, which is incorporated into their axial stiffness.

Following the previous studies (De Biagi and Chiaia, 2013; De Biagi, 2016), the deformation work W in linear elastic systems was employed as functional in investigating the problem and performing the analysis. The damage propagation was conceptualized as a gradual reduction of the element's stiffness from its initial value to zero; in this way the progressive removal of the element was effectively represented. Considering the arbitrary qth rod, which undamaged stiffness is k_q, the damage was mathematically included through the Lemaître and Chaboche formulation as a reduction of the axial stiffness $k_{q,\xi}$

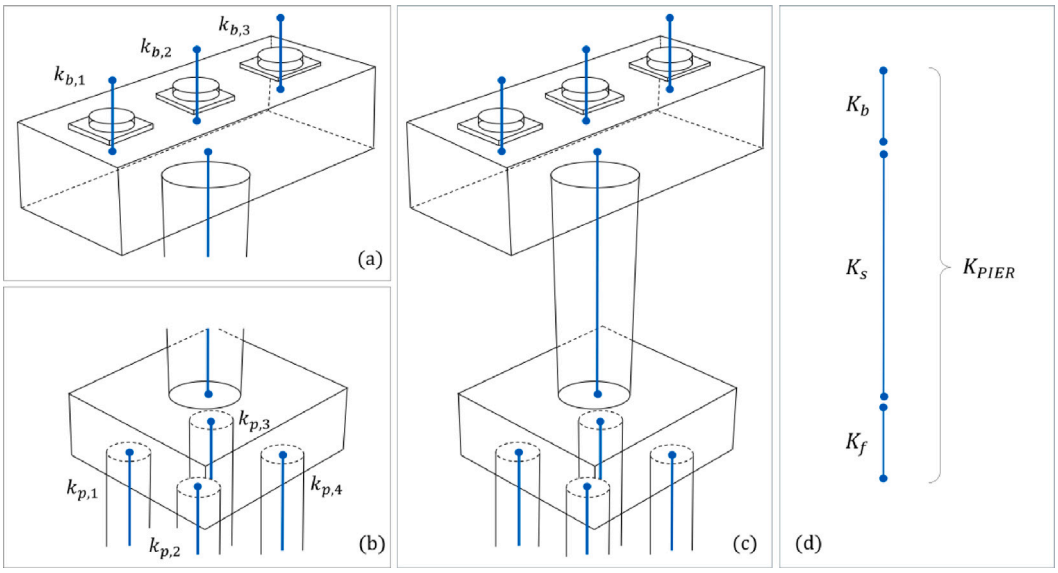

Fig. 1. Example 1. Pier's structural element layout comprising its individual components. (a) Bearing support system. The support system of the pier consists of the bearings devices working in parallel with each other; (b) foundation system. The foundation system of the pier consists of the foundation piles working in parallel with each other; (c) the structural components of the pier: bearing support system, shaft and foundation system work in series with each other; (d) schematization of the pile's components working.

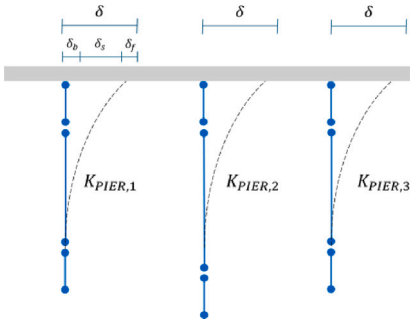

Fig. 2. Bridge superstructure with three piers.

as (Lemaitre and Chaboche, 1994):

$$k_{q,\xi} = k_q\,(1-\xi)\,. \tag{6}$$

The quantity ξ is the damage variable ranging from 0 (undamaged state) to 1 (totally removed element). Element damage presupposes a negative variation of the stiffness with respect to damage increment.

The application of Clapeyron's Theorem (Carpinteri, 1992) allows to assess the deformation work experienced by a linear system under the application of an external force F. The elastic work of deformation of the system can be easily calculated as:

$$W = \frac{1}{2}F\delta = \frac{1}{2}\frac{F^2}{K_{eq}}, \tag{7}$$

It is possible to determine the overall stiffness of the entire system, denoted as equivalent stiffness K_{eq}, depending on the position of the single elements. A perturbation in the stiffness of one rod implies a variation in the system's equivalent stiffness, thus, leading to a change in the elastic work of deformation (Belluzzi, 1946; Carpinteri, 1992).

Differently from previous studies, the present study focused not only on the first derivative of the deformation work (with respect to the damage variable), but also on the trend of the increment, i.e., the second derivative, as a potential information on load transfer mechanisms that occur on the structure. In addition to De Biagi's studies, this analysis examined the trends in the variation of deformation work. The variation of the elastic deformation work ∂W due to a change in the stiffness of the qth rod, was computed by differentiating Eq. (7) with respect to the k_q:

$$\frac{\partial W}{\partial k_q} = \frac{F^2}{2}\frac{\partial}{\partial k_q}\left(\frac{1}{K_{eq}}\right). \tag{8}$$

The derivative of W with respect to the damage variable was obtained from the chain rule for differentiating composite functions:

$$\frac{\partial W}{\partial \xi} = \frac{\partial W}{\partial K_{eq}}\frac{\partial K_{eq}}{\partial k_{q,\xi}}\frac{\partial k_{q,\xi}}{\partial \xi}. \tag{9}$$

It is worth to note that the first two terms in the derivations chain reported in Eq. (9) are the derivative of W with respect to the change of the stiffness of the qth rod, while the last term refers to the model adopted to include the damage, i.e. Eq. (6). This presupposes that an additional derivative, non dependent from the damage variable, can describe the system:

$$\frac{\partial W}{\partial k_q} = \frac{\partial W}{\partial K_{eq}}\frac{\partial K_{eq}}{\partial k_q}. \tag{10}$$

In the latest situation, the derivative reflects the actual state of the system, independently from the evolution of the damage. Briefly, one can obtain the same k_q by having a large damage on a stiff rod or, similarly, a small damage on a weak rod. The key idea is that both scenarios (a stiff rod with large damage and a weak rod with small damage) can result in the same stiffness (k_q). This means that despite their different conditions and histories of damage, these structures exhibit similar behavior in terms of stiffness. Therefore, it is possible to group them into a *family* of structures because the same situation reflects similar structures. Structures in the same family share the same value of stiffness; different families share the same step of damage, but resulting in different values of the actual stiffness of the damaged element as the initial conditions (undamaged stiffness) differs family-by-family. This approach helps in understanding and analyzing structures with varied damage but similar mechanical responses.

To summarize, the approach to the problem is twofold: by inducing the damage to a single structure or by examining multiple similar structures with varying levels of rod stiffness, thus forming a set of families of structures, to simulate the damaging process.

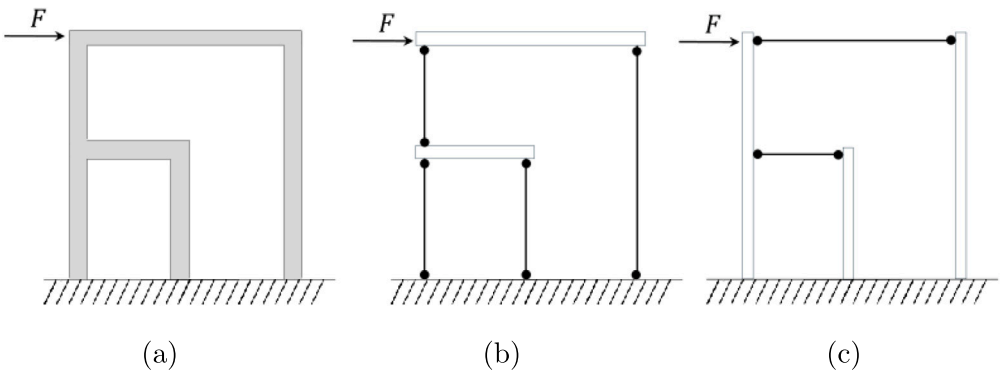

Fig. 3. (a) Shear-type frame subjected to horizontal loading F; (b) Shear-type frame schematization under the hypothesis of infinitely rigid floors; (c) Flexure-type frame schematization under the hypothesis of infinitely rigid vertical elements.

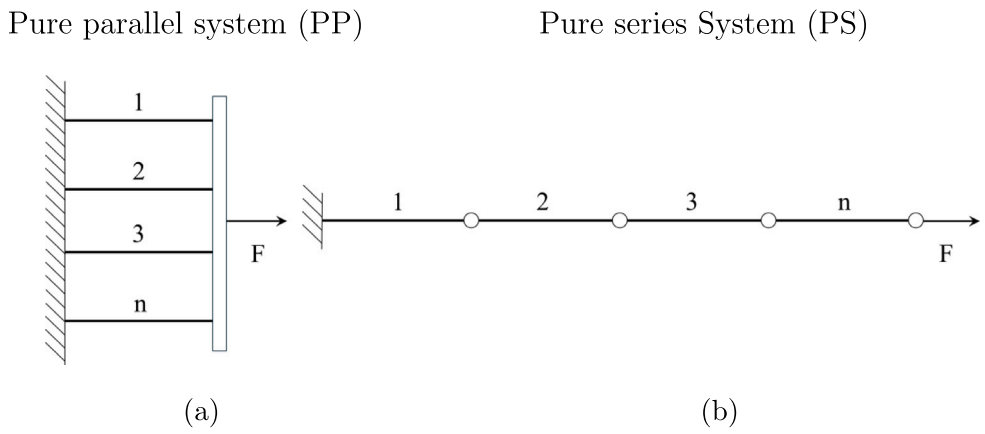

Fig. 4. Systems of rods: (a) pure parallel system (PP); (b) pure series system (PS).

3.1. Analytical formulations

In the following paragraph the detailed method formulations for the configuration of pure parallel (PP), pure series (PS) and mixed (MIX) system, are introduced.

The static equilibrium of elastic systems is defined by the balance between internal forces and externally applied forces, depending on the arrangement of the elements. In the PP system, the n rods are arranged in parallel, Fig. 4.(a), in the PS system the n rods are arranged in series, Fig. 4.(b). A further arrangement considering that some parts are in parallel and others in series is introduced.

3.1.1. Pure parallel system (PP)

In pure parallel (PP) case, the right-hand side end is connected to a rigid body to which an external force F is applied, remaining equal during the entire process; the left-hand side ends are constrained and the displacements are prohibited. The rotational degree of freedom and displacements along the vertical direction are not allowed. The equivalent stiffness of the PP system is given by the direct sum of each rod stiffness contribution:

$$K_{eq}^{PP} = k_1 + k_2 + k_3 + \cdots + k_n = \sum_{i=1}^{n} k_i. \tag{11}$$

The rod perturbation is introduced and the damage condition on the qth rod is thus simulated. The equivalent stiffness is rewritten as:

$$K_{eq}^{PP}(k_q) = \left(\sum_{i=1}^{n} k_i - k_q\right) + k_q. \tag{12}$$

The elastic work of deformation of the system of rods, W, is computed through Clapeyron's Theorem (Carpinteri, 1992) and is expressed as:

$$W = \frac{1}{2} F\delta = \frac{1}{2} \frac{F^2}{\left(\sum_{i=1}^{n} k_i - k_q\right) + k_q}. \tag{13}$$

Considering that the qth rod can vary its stiffness during the damage process according to the damage model reported in Eq. (6), Eq. (13) can be rewritten as:

$$W = \frac{1}{2} \frac{F^2}{\left(\sum_{i=1}^{n} k_i - k_q\right) + k_{q,\xi}}. \tag{14}$$

Hence, the variation of the elastic work of deformation, ∂W, due to a variation of the stiffness of the qth rod, $\partial k_{q,\xi}$, is computed by differentiating Eq. (14) and is equal to:

$$\frac{\partial W}{\partial k_{q,\xi}} = -\frac{F^2}{2} \frac{1}{\left[\left(\sum_{i=1}^{n} k_i - k_q\right) + k_{q,\xi}\right]^2}, \tag{15}$$

showing that a decrease in stiffness always produces increments of the work of deformation.

To examine the evolution of the elastic work of deformation, ∂W, during the damage process, $\partial\xi$, Eq. (15) is differentiated with respect to the damage variable ξ, obtaining:

$$\frac{\partial W}{\partial \xi} = \frac{F^2}{2} \frac{k_q}{\left[\left(\sum_{i=1}^{n} k_i - k_q\right) + k_q\,(1-\xi)\right]^2}, \tag{16}$$

which is positive. The derivations of the formulae are further detailed in Appendix A.

3.1.2. Pure series system (PS)

In the pure series (PS) case the right-hand side of last rod is subjected to an external horizontal force F, that is kept fixed across the whole analysis; the left-hand side end of first rod is constrained and its displacements and rotations are prohibited. The equivalent stiffness of the PS system is given by the inverse of the sum of the inverses of each

stiffness element, as:

$$K_{eq}^{PS} = \left[\frac{1}{k_1} + \frac{1}{k_2} + \cdots + \frac{1}{k_n}\right]^{-1} = \left[\sum_{i=1}^{n} \frac{1}{k_i}\right]^{-1}. \tag{17}$$

The rod perturbation is introduced and the damage condition on the qth rod is thus simulated. The equivalent stiffness is rewritten as:

$$K_{eq}^{PS} = \left[\left(\sum_{i=1}^{n} \frac{1}{k_i} - \frac{1}{k_q}\right) + \frac{1}{k_q}\right]^{-1}. \tag{18}$$

The term in the curved brackets is considered as the inverse of the equivalent stiffness of the system without the contribution of the qth rod, i.e., $K_{\text{eq},-q}$:

$$\frac{1}{K_{\text{eq},-q}} = \sum_{i=1}^{n} \frac{1}{k_i} - \frac{1}{k_q}. \tag{19}$$

Rearranging the terms, the equivalent stiffness of the PS system is:

$$K_{eq}^{PS} = \left(\frac{k_q + K_{\text{eq},-q}}{k_q K_{\text{eq},-q}}\right)^{-1}. \tag{20}$$

The elastic work of deformation, computed through Clapeyron Theorem, is:

$$W = \frac{F^2}{2}\left(\frac{k_q + K_{\text{eq},-q}}{k_q\ K_{\text{eq},-q}}\right)^{-1}, \tag{21}$$

and the variation of the elastic work of deformation with respect to the damage is:

$$\frac{\partial W}{\partial \xi} = \frac{F^2}{2} \frac{\left(k_{q,\xi}\ K_{\text{eq},-q}\right) - \left(K_{\text{eq},-q} + k_{q,\xi}\right) K_{\text{eq},-q}}{\left(K_{\text{eq},-q}\ k_{q,\xi}\right)^2} k_q. \tag{22}$$

The derivations of the formulae are further detailed in Appendix B.

3.1.3. Series–parallel system (MIX)

The structural complexity refers to structures made up by a large number of parts that interact in a non-simple way (De Biagi, 2018). In the case of statically determined structures, the load path is unambiguously identified and the problem of how the load redistribution occurs within the structures does not arise. In statically indeterminate structures, which are prevalent in many structural applications, the redistribution of the load paths remains an uncertain factor. In such situations, each element contributes differently to the functioning of the overall system (Shokrollahi and Zayeri Baghlan Nejad, 2014). However, the effective contribution of each element cannot be precisely determined. Following previous researches, when the participation of all the load paths is equally effective, the structure reaches the maximum complexity. On the contrary, if all the load paths except one are effective, the structure is called as non-complex or "simple" (De Biagi and Chiaia, 2013).

With the specific purpose to introduce the complexity in the system, a configuration of interconnected rods arranged in both series and parallel configurations is showcased in Fig. 5. In the following, the Authors refer to the system as mixed system (MIX). The system is statically indeterminate with an order of indeterminacy of 4.

In this case, the evaluation of the equivalent stiffness K_{eq} becomes more complex compared to the straightforward cases of PP and PS systems. When the configuration is not purely parallel or purely series, a combination of these fundamental configurations within nested levels is expected. In this case, the resulting equivalent stiffness for the MIX system is expressed as:

$$K_{eq}^{MIX} = \frac{k_1k_3 + k_1k_4 + k_2k_3 + k_2k_4 + k_3k_4}{k_1 + k_2 + k_3}. \tag{23}$$

The rod perturbation is introduced. As an example, we consider that the damage progresses on Rod #1. As performed in the previous paragraphs, the elastic work of deformation W is derived with respect to the damage variable acting on Rod #1, resulting in:

$$\frac{\partial W}{\partial \xi} = \frac{F^2}{2}\left[\frac{(-A + BC)k_q}{(A + Bk_{q,\xi})^2}\right], \tag{24}$$

with $A = k_2k_3 + k_2k_4 + k_3k_4$, $B = k_3 + k_4$, and $C = k_2 + k_3$. A similar approach can be obtained if the damage is applied to the other rods. In-depth details of the formulations can be found in the Appendix C.

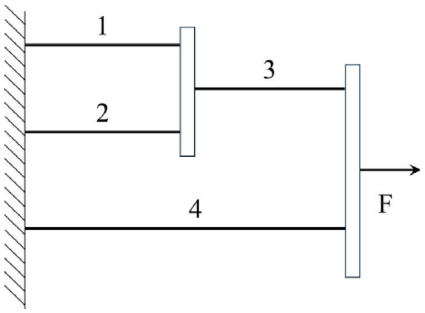

Fig. 5. In the series–parallel system, herein named as mixed system (MIX), the rods are arranged in both series and parallel configurations. The system has an order of indeterminacy of 4.

4. Results

In this section, various results for the pure parallel (PP), mixed (MIX), and pure series (PS) systems are presented. The results were generated by considering the three systems PP, MIX and PS in which rods #2, #3 and #4 have stiffnesses equal to 1, 2 and 1, respectively. It is important to note that, for the purposes of the analyses, the values of the stiffnesses are normalized to a reference value. Ten different initial structures are simulated, with Rod #1 taking values between 0 and 5. The numbering of the elements is the one reported in Figs. 4 and 5. Fig. 6 reports the values of $\partial W/\partial \xi$ for the three systems (PP, PS and Mixed) and for the 10 different initial configurations, i.e., the value of k_1 with respect to the damage parameter ξ in the range 0 to 1 for PP and MIX systems, and in the range 0 to 0.9 for PS system. As mentioned, the complete removal of Rod #1 (i.e. a damage variable equal to 1) is not possible since the system becomes unconnected.

Interesting results are observed in Fig. 6. Starting by describing the trends of the two extreme cases, for pure parallel (a) an increase in the damage level ξ results in an increase in the derivative of the deformation energy. A similar trend occurs for the pure series system (c). However, their distinction lies in the fact that as the stiffness of the rod under damage decreases, in the case of pure parallel (a), the variation of internal energy decreases (the curves trend downward), whereas in the case of pure series (c), the variation of internal energy increases (the curves trend upward). As a matter of fact, the dashed violet curve representing the damaging process of a structure with $k_1 = 5$, is the highest curve above all the set in the pure parallel system. That means, for a given level of damage, the curves trend downward by decreasing the rod stiffness. The same dashed violet curve representing the damaging process of rod of a pure series system with $k_1 = 5$ is the lowest curve at the bottom of the set. That means, for a fixed level of damage, by decreasing the rod stiffness the curves trend upward. In the case of the mixed system (b) an increase in the damage level ξ results in an increase in the derivative of the deformation energy, as occurs in the previous cases described above. However by decreasing the rod stiffness, the curves trend is not constant: considering a large damage level, e.g. $\xi \approx 0.9$, the values of $dW/d\xi$ increase for increasing k_1. For smaller damage levers, e.g. $\xi \approx 0.1$, the previous trend is not observed anymore. It seems that the value of $dW/d\xi$ increases for k_1 from 0 to 2.0, while it decreases for values of k_1 larger than 2.0, with a maximum at around 2.0. The plots of Fig. 6 were annotated to highlight these

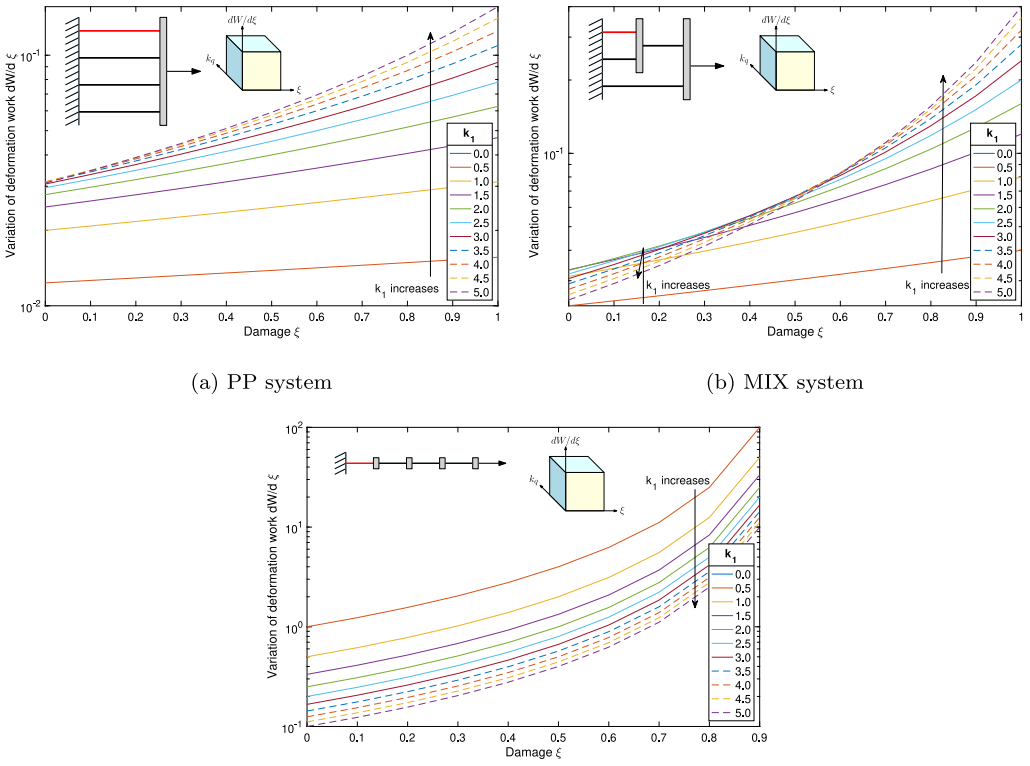

(a) PP system

(b) MIX system

(c) PS system

Fig. 6. Effects of the damage parameters ξ on the value of $\partial W/\partial\xi$. The damage acts on the Rod #1 on a pure parallel system (a), mixed system (b) and pure series system (c). For each system, different values of the initial stiffness of Rod #1 are considered. Note that the curve related to $k_1 = 0$ does not exist in a pure series system (c).

trends.

The analysis of the curves in the previous sections follows the standard approach for evaluating the effects of damage on a system, starting from the damage parameter value. However, a detailed examination reveals an interesting property. According to Eq. (9), the derivative of W can be expressed as a product of various terms, including $\partial k_{q,\xi}/\partial\xi$, which equals $-k_q$. This indicates that the curves represent the evolution of a structure where the stiffness of the qth rod changes, yet retains a memory of its initial stiffness.

To clarify, consider the following two scenarios:

1. A scheme (PP, MIX, or PS indifferently) where the qth rod has an initial stiffness of 10, and the damage parameter ξ reaches 0.5. The "damaged" stiffness is then 5.
2. A scheme where the qth rod has a stiffness of 5 with no damage applied.

In both cases, the qth rod ends up with a stiffness of 5, but the resulting derivative $\partial W/\partial\xi$ differs between the two scenarios.

Following this consideration, the same set of results can be analyzed in a complementary way. The curves of Fig. 6 represent a family of initial values of stiffness k_q for the rod under damage. Each curve of the three subplots represent a different initial structure, with Rod #1 having a different initial value. At any fixed point on the axis of the abscissae (that is the damage axis), the variations among the curves can be closely examined. Observing how the curves change upwards and downwards allows to understand how the variation in the stiffness of the rod influences the derivative of the deformation work, thereby tracking the progression of damage. Consequently, the damage process can be interpreted as a function of the stiffness variation.

The results reveal interesting pattern in the curves. If the results are analyzed with a focus on the individual curve, say for example the curve related to $k_1 = 5$ in Fig. 6.(a), an increase in damage always corresponds to an increase of the increment of deformation work, in all the three cases (parallel, series and mixed). On the other hand, if the results are analyzed through the curves, across multiple stiffness families at a fixed ξ-coordinate, the outcome is not always trivial. It has been observed, in fact, that in systems where the rods are arranged in pure parallel (PP), a decrease in the rod stiffness leads to a negative change in deformation work (the curves exhibit a downward trend) as shown in Fig. 6.(a); conversely, in systems with rods arranged in pure series (PS), a decrease in the rod stiffness results in a positive change in deformation work (the curves exhibit an upward trend) as depicted in Fig. 6.(c). This outcome becomes particularly significant when the parallel and series systems are combined (MIX system). From Fig. 6.(b) it can be seen that, in fact, the curve trend is mixed. For certain stiffness values of the rod under damage, the variation has positive value (it increases), while for others, the variation is negative (it decreases). Fig. 7 illustrates the concept highlighting the values of the derivative of the deformation work at a null damage level. It is seen that the purple curve, named in the following as $\Omega(k_1)$ is not monotonic, with a maximum.

This finding is crucial because it indicates that for the same geometric configuration, the whole system can operate in a series-regime for certain stiffness values of the under damage rod, and in a parallel regime for others, as reported in the following. This reveals that the elements geometric arrangement alone does not necessarily predict the behavior of the structure; instead, it is determined by the linear stiffness combination of the rods. Thus, stating that the system's rods are arranged in parallel does not guarantee that the system is working in parallel. This phenomenon can be better observed by switching to a coordinate system where the variation in stiffness on a mixed system is measured on the abscissa as in Fig. 8. For sake of clarity, we name as Ω the value of the variation of the deformation work with respect to the damage variable, i.e. $\partial W/\partial\xi$, when the damage variable has a given value. In particular we consider the undamaged situation, where

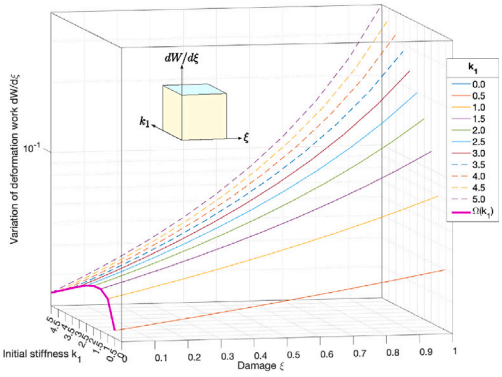

Fig. 7. Mixed system with Rod #1 having a stiffness in the range 0 to 5. The trend of the variation of deformation work $dW/d\xi$ corresponding to a damage value $\xi = 0$ is highlighted in purple.

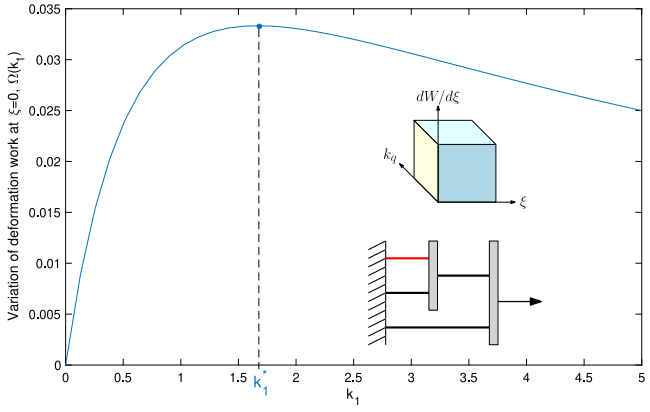

Fig. 8. Mixed system with Rod #1 having a stiffness in the range 0 to 5. The value of $\Omega(k_1)$ is plotted versus the value k_1. The behavior results in a bell-shaped curve. For certain stiffness values of the Rod #1, $d\Omega/dk_q > 0$, while for others, it decreases $\partial\Omega/\partial k_q < 0$.

$\xi = 0$, resulting in:

$$\Omega\left(k_q\right) = \left\| \frac{\partial W}{\partial \xi} \right\|_{\xi=0}. \tag{25}$$

Fig. 8 represents the trend of Ω for k_q, here the stiffness of Rod #1, in the range 0 to 5. It can be observed that the variation of deformation work presents a bell-shape trend, with a peak at k_1^*. As detailed in the following, this value corresponds to a transition between regimes on the structure.

In Fig. 9, the results of stiffness variation in Rod #1, Rod #3 and Rod #4 are compared. The three different values of k^* and ∂W peaks are obtained. It is observed that modifying the stiffness or removing Rod #3 induces a significantly larger change compared to acting on Rod #4 and Rod #1. The discrepancy is of an order of magnitude. When the stiffness of the rod under modification exceeds unit value, the system operates in series, as it dominates the behavior. Conversely, when the stiffness values drop to the unit value and below, the system operates in parallel, indicating cooperative behavior among all the rods.

To further stress the finding, another comparative example is proposed. Consider three different distribution of initial stiffnesses in a mixed system:

- Configuration (A) $k_1 = 1, k_2 = 1, k_3 = 2$, and $k_4 = 1$;
- Configuration (B) $k_1 = 1, k_2 = 2, k_3 = 2$, and $k_4 = 1$;
- Configuration (C) $k_1 = \frac{1}{2}, k_2 = \frac{2}{3}, k_3 = 2$, and $k_4 = 1$.

Table 1
Results of the analysis of the damage cases.

Parameter	Rod #1	Rod #2	Rod #3	Rod #4
Case A				
k	1	1	2	1
k_q^*	1.6552	1.6552	0.6897	0.125
$\Omega\left(k_q^*\right)$	0.0333	0.0333	0.0332	0.9796
Case B				
k	2	2	1	1
k_q^*	2.6000	2.6000	0.7347	1.2245
$\Omega\left(k_q^*\right)$	0.0208	0.0208	0.8437	0.1042
Case C				
k	1/2	3/2	2	2
k_q^*	1.3469	1.1110	0.5510	0.7347
$\Omega\left(k_q^*\right)$	0.0417	0.04759	0.0916	0.1696

Fig. 10 depicts the value of $\Omega\left(k_q\right)$ for the three configurations by varying the stiffness of the single rods in the range [0;3]. Each plot contains the curves related to the Rods #1, 3 and 4. Rod #2 has the same curve as Rod #2. To explain how the curves have been determined, the blue curve of Configuration A plot is obtained setting $k_1 = k_2 = 1$ and $k_4 = 1$ and varying k_3 in the range [0;3]. Briefly, the rods that are not affected by the variation are set equal to the initial stiffnesses previously listed for each configuration, further indicated in Table 1. The red curve represents the variation of Rod #1, the blue curve refers the variation of Rod #3, while the green curve represents the variation of Rod #4.

Considering Configuration A, Fig. 10.(a), when Rod #1 is modified, the critical stiffness k_1^* is 1.6552. For higher stiffness values, the system operates in series, and thus the responding system is composed of Rods #1-#2-#3. For lower stiffness values, the system operates in parallel, and thus the responding system encompasses the entire system. This is reasonable. Considering the SP-system under the horizontal load, it consists of two subsystems: Subsystem 1 (SS1: #1, #2, and #3) and Subsystem 2 (SS2: #4). These two subsystems operate in parallel with each other. For $k_1 = 1.6552$, the equivalent stiffness of SS1 is 1.14, and that of SS2 is 1. Thus, it is evident that for values of rod stiffness k_1 greater than 1.6552, Subsystem 1 dominates, resulting in the series regime of rods #1-#2-#3.

Consider Configuration C, Fig. 10.(c), when Rod #4 is perturbed, the critical stiffness, k_4^*, is 0.7347. For higher values, the system operates in series, therefore the responding system consists solely of Rod #4. For lower values, the system operates in parallel, thus including the entire structure in the response. This result is in alignment with the conducted analysis. At a stiffness value $k_4 = 0.7347$, the Subsystem 1 (SS1: #1, #2, and #3) has an equivalent stiffness of 0.74, while Subsystem 2 (SS2: #4) has a stiffness of 0.7347. Consequently, for stiffness values of Rod #4 greater than 0.7347, Subsystem 2 prevails, leading to a series mechanism dominated by the single Rod #4. Similar reasoning can be applied to Case B, which results are reported in Fig. 10.(b).

5. Discussion

The analytical results presented in this study highlight significant findings concerning the behavior of complex systems under varying conditions of damage or, similarly, under perturbation of the stiffness of their components.

Analyzing individual curves reveals that increased damage consistently corresponds to an increase in deformation work across all configuration systems (parallel, series, and mixed). However, examining results across different stiffness families at a fixed ξ-coordinate reveals non-trivial outcomes. Specifically, in a coordinate system where

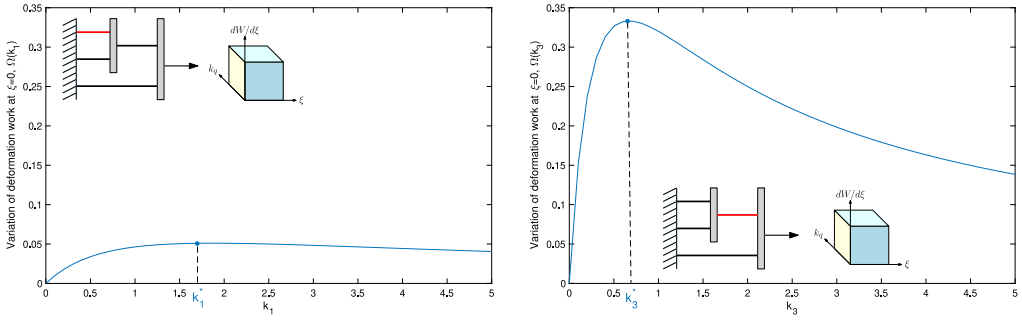

(a) Rod #1 (b) Rod #3

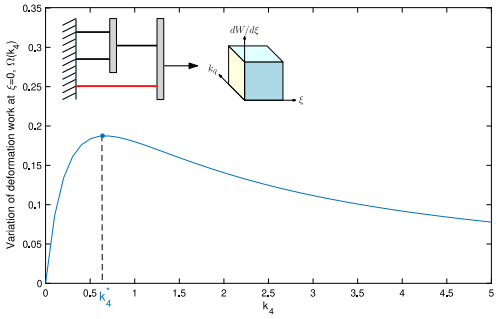

(c) Rod #4

Fig. 9. Values of $\Omega(k_q)$ on a mixed system for different values of the stiffnesses of rods #1, 3 or 4.

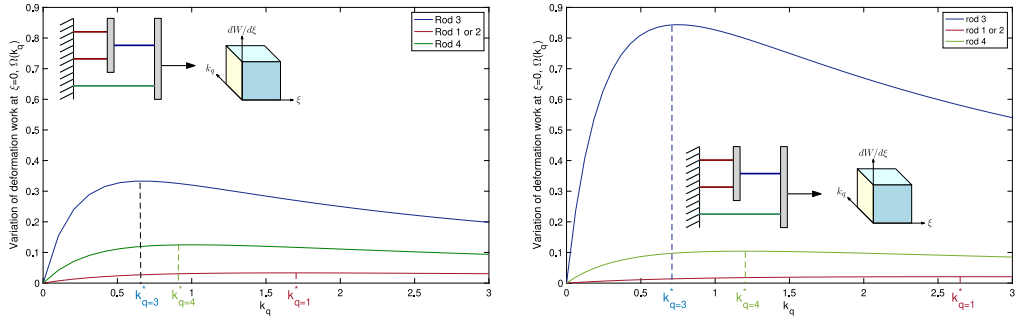

(a) Case A (b) Case B

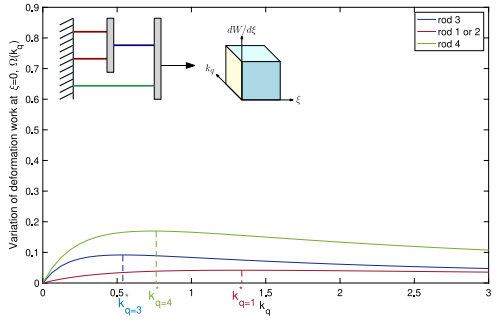

(c) Case C

Fig. 10. Values of $\Omega(k_q)$ on a mixed system. The bell-shaped red curve depicts the value of $\Omega(k_1)$, i.e. the stiffness of Rod #1 changes, the blue curve refers to †, i.e. $\Omega(k_3)$, and the green curve refers to Rod #4, i.e. $\Omega(k_4)$. The three Configurations (A, B, C) are considered.

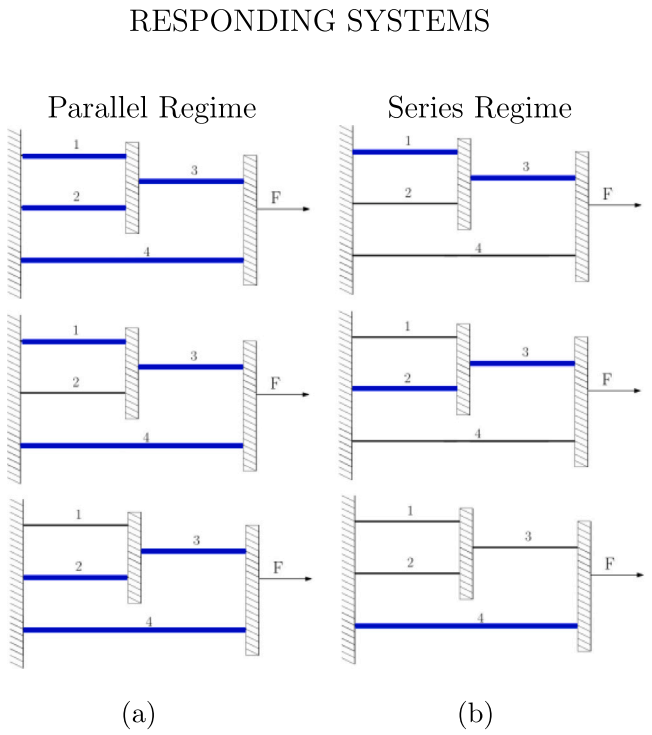

Fig. 11. Mixed systems: (a) Systems working in parallel regime (b) Systems working in series regime.

damage progression is measured on the abscissa and internal energy variation on the ordinates, pure parallel rod arrangements (PP) show that a decrease in rod stiffness leads to negative changes in deformation work (evidenced by a downward trend in curves). Conversely, in pure series rod arrangements (PS), decreasing rod stiffness results in positive changes in deformation work (evidenced by an upward trend in curves). To better understand this concept, a new variable was introduced to represent the change in deformation work when the damage variable has a fixed value, i.e. $\xi = 0$. The variation of deformation work across different stiffness values, plotted with stiffness on the abscissa, results in a bell-shaped curve. Based on the distribution of stiffness in the rods, for certain stiffness values of a rod under damage it results $d\Omega/dk_q > 0$, indicating an increase in deformation work, while for others, $d\Omega/dk_q < 0$, indicating a decrease in deformation work.

This outcome becomes crucial in the case of mixed systems where both series and parallel arrangements are combined. Depending on the stiffness distribution in the rods, it is possible to find a critical stiffness k_q^*. For stiffness values greater than k_q^*, the system will behave as a series arrangement, while for values less than k_q^*, the system will behave as a parallel arrangement. The results evidence that the same geometrical system can operate in both series and parallel regime (Fig. 11), depending on the overall stiffness distribution within the system. The geometric arrangement of elements alone do not predicts the structural behavior of the system. The proposed analysis facilitate the mapping of the load paths variation within the system in ongoing damage scenario. This phenomenon is evident in the bell-shaped trend of deformation work variation when the stiffness variation in plotted on the abscissa. Lastly, comparing the effects of applying damage to rods positioned in different places, the value of the variation in deformation work, hence its magnitude, serves as an indicator of the impact of removing one rod compared to another.

Finally, two important findings can be extracted.

- The parameter $\Omega(k_q)$ allows for the identification of the critical stiffness value k_q^*, at which the system behaves in series or in parallel. This helps determine whether the element is part of the preferential load path (series behavior) or not (parallel behavior) for specific stiffness values, thus, the working regime.
- Mapping the parameter $\frac{\partial W}{\partial \xi}$ allows for the visualization of the variation in the load path during the damage of a random element within the structure. Specifically, it identifies which elements are loaded and which are unloaded.

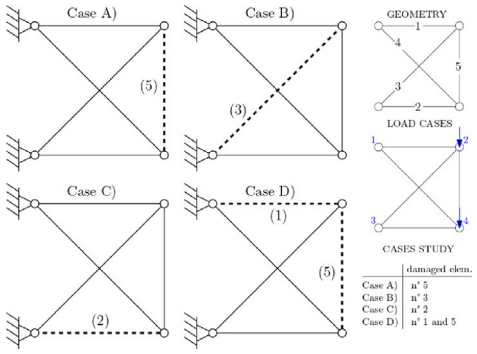

Fig. 12. Case studies. Case (A) damage to element no. 5; Case (B) damage to element no. 3; Case (C) damage to element no. 2; Case (D) damage to elements no. 1 and no. 5. Basic information on the geometry is provided on the right-hand side. There are 2 load cases: Load Case 1: vertical force F applied at node 2; Load Case 2: vertical force F applied at node 4.

6. Application to a basic truss structure

In the previous section, the attention focused on gaining a deeper understanding of the parameter $\Omega(k_q)$ as a metrics to understand if there is a transition in the behavior of the system as a modification on the stiffness of the components occurs, i.e. a transition in the behavior of the system. In addition, the parameter serves to define, given a set of elements' stiffness, which elements are predominant in the load path and which are negligible. In this section, the focus shifts to a deeper understanding on the variation of the strain energy on the single elements with respect to the damage parameter, to demonstrate the dual significance and effectiveness of the method.

A simple 2D truss example made of a single-module is considered, as sketched in Fig. 12. The structure consists of 4 nodes and 5 bar elements: an upper and a lower chords, two members forming the cross-bracing (St. Andrew's cross), and a vertical member. The initial cross-sectional area of the members is set at 0.05 m^2, the Young's modulus $E = 210 \times 10^9$ Pa. Vertical and horizontal members are 1 meter long, while the diagonal bracing members are 1.4142 meters long.

To determine the level of statically indeterminacy of the structure, the following formula (Gere and Goodno, 2012) has been used:

$$I = m + r - 2j, \tag{26}$$

where I is the degree of static indeterminacy, m is the number of members (elements), r is the number of external restraints (fixed degrees of freedom), and j is the number of joints (nodes). In this case: $j = 4$, $m = 5$; node 1 and 3 are fully fixed, each with 2 restraints (horizontal and vertical), therefore $r = 4$. It results: $I = m + r - 2j = 5 + 4 - 2 \times 4 = 9 - 8 = 1$. Thus, the structure is characterized by one level of static indeterminacy.

Two load cases are considered: a force F of 1 kN is vertically applied at top right node (Node 2, Load Case 1) or alternatively at bottom right node (Node 4, Load Case 2). The structure is subjected to a damage consisting on the reduction of the cross-sectional area of selected elements of about 10%. Four damage cases are studied: Case (A) involves the progressive failure of the vertical member 5; Case (B) involves the progressive failure of the bracing element 3; Case (C) involves the progressive failure of the lower chord 2; Case (D) involves

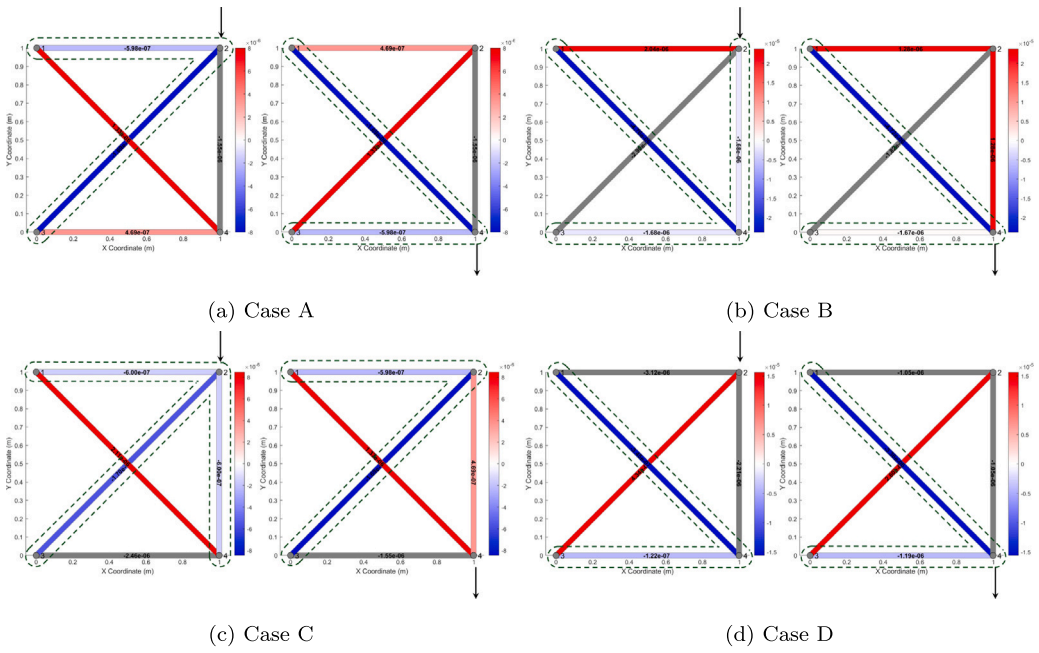

Fig. 13. Cases study results for Case (A), (B), (C), and (D). For each case, the left-hand side plot corresponds to Load Case 1, the right-hand side plot to Load Case 2. The graphs present the result in the form of a color-map, which maps the variation in deformation work, indicating that negative variations (blue elements) correspond to elements being loaded, while positive variations (red elements) correspond to elements being unloaded. The element under damage is indicated in gray. The dashed line represents the alternative load path that originates as a consequence of the damage to a random element.

the simultaneous progressive failure of elements 1 and 5 (Fig. 12).

To analyze the effects within the system and investigate how the redistribution of load paths varies as the evolution of damage propagation advances, the term $\partial W_i/\partial k_j$ representing the variation of strain energy on the ith rod due to the modification on the stiffness of the kth rod was numerically computed rod-by-rod.

It is worth noting that a negative value of $\partial W_i/\partial k_j$ represents an increase in internal energy on the element as the stiffness k_j reduces to simulate a damage. A positive derivative for a reducing k_j represents a decrease in the internal energy. These two conditions are depicted in the color-maps in Fig. 13 and, in particular, the elements marked in blue (characterized by negative derivative values) experience an increase of the deformation work, while elements in red a decrease of W_i. Therefore, depending on the damage to the specific element of each case, the blue color indicates that the element is being loaded, while the red color represents a reduction of load in that element. In conclusion, by mapping the variation in deformation work through color maps that distinguish between positive and negative increments, the evolution of load paths within the structure during the progressive damage of an element can be immediately visualized. The alternative load path that originates as a consequence of the damage to an element are shown in Fig. 13 with dashed lines. The obtained results are in agreement with the redistribution of forces in statically determined trusses.

7. Conclusions

Series and parallel component configurations are widely implemented in various fields and engineering disciplines, nevertheless their formal integration within mechanical and structural engineering, particularly in terms of a structured framework for metrics and theoretical models describing load transmission, remains undeveloped.

In this study, the analysis of rod systems in the case of pure parallel (PP), pure series (PS) and the mixed (MIX) elements arrangement have been proposed. The damage procedure has been analyzed with two different approaches of stiffness progressive reduction. The functional is the variation of deformation work. Analyzing the variation of the deformation work of the system during a random element under damage, it is possible to identify the working regime behavior of the system. Although formulated for linear elastic systems, the proposed approach provides a theoretical model to analyze how damage distribution in rod systems significantly influences load paths and the overall structural response. The analysis highlighted that the location and extent of damage can drastically alter the regime behavior of the rod systems. The proposed metrics has been further applied to a more complex system to show the capacity of the approach to highlight the load paths in non-trivial structures. These insights contribute to a larger study focused on optimizing sensor placement, using this method to monitor shifts in load paths and identify when specific elements become integral to the primary load-bearing path as damage progresses in random structural elements. This approach has the potential to be a key strategy for designing effective monitoring systems, with promising results already emerging from ongoing research.

CRediT authorship contribution statement

Lorenza Abbracciavento: Writing – review & editing, Writing – original draft, Methodology, Investigation, Formal analysis, Data curation, Conceptualization. **Valerio De Biagi:** Writing – review & editing, Writing – original draft, Supervision, Methodology, Investigation, Formal analysis, Data curation, Conceptualization.

Declaration of competing interest

The authors declare that they have no known competing financial interests or personal relationships that could have appeared to influence the work reported in this paper.

Acknowledgments

The authors gratefully acknowledge the support provided by the European Union and the Italian Ministry of University and Research through the plan “Italia Domani, Piano Nazionale di Ripresa e Resilienza”. This publication was produced while L.A. is attending the PhD at Politecnico di Torino, with the support of a scholarship co-financed by MUR - DM 352/2022 (Ministerial Decree No. 352 dated

April 9, 2022) (NRRP - funded by the European Union - NextGenerationEU - Mission 4 “Education and Research”, Component 2 “From Research to Business”, Investment 3.3), and by RAV, Raccordo Autostradale Valle d’Aosta.

Appendix A. Pure parallel system

The equivalent stiffness of a system of rods in parallel is provided by:

$$K_{eq}^{PP} = k_1 + k_2 + k_3 + \cdots + k_n = \sum_{i=1}^{n} k_i. \tag{A.1}$$

The total stiffness can be rewritten based on the qth element as:

$$K_{eq}^{PP}(k_q) = \left(\sum_{i=1}^{n} k_i - k_q\right) + k_q. \tag{A.2}$$

The total work of deformation, considering the linear elasticity, is:

$$W = \frac{1}{2} F\delta = \frac{1}{2}\frac{F^2}{K_{\text{eq}}^{PP}(k_q)} = \frac{1}{2}\frac{F^2}{\left(\sum_{i=1}^{n} k_i - k_q\right) + k_q}. \tag{A.3}$$

The Lemaître and Chaboche formulation for the stiffness of the qth rod is:

$$k_{q,\xi} = k_q\,(1-\xi), \tag{A.4}$$

where $k_{q,\xi}$ is the reduced stiffness, ξ is the damage parameter, and k_q is the undamaged value of the stiffness of the qth rod.

Considering that the qth rod can vary its stiffness during the damage process according to the damage model reported in Eq. (A.4), Eq. (A.3) can be rewritten as:

$$W = \frac{F^2}{2}\frac{1}{\left(\sum_{i=1}^{n} k_i - k_q\right) + k_{q,\xi}}. \tag{A.5}$$

Hence, the variation of the elastic work of deformation, ∂W, due to a variation of the stiffness of the qth rod, $\partial k_{q,\xi}$, is computed by differentiating Eq. (A.5) and is equal to:

$$\frac{\partial W}{\partial k_{q,\xi}} = -\frac{F^2}{2}\frac{1}{\left[\left(\sum_{i=1}^{n} k_i - k_q\right) + k_{q,\xi}\right]^2}. \tag{A.6}$$

Considering the derivation rule of composite functions, i.e.,

$$\frac{\partial W}{\partial \xi} = \frac{\partial W}{\partial k_{q,\xi}}\frac{\partial k_{q,\xi}}{\partial \xi}, \tag{A.7}$$

and recalling that the variation of $k_{q,\xi}$ with respect to the damage variable is:

$$\frac{\partial k_{q,\xi}}{\partial \xi} = -k_q, \tag{A.8}$$

the variation of the total work with respect to the damage parameter results in:

$$\frac{\partial W}{\partial \xi} = \frac{F^2}{2}\frac{k_q}{\left[\left(\sum_{i=1}^{n} k_i - k_q\right) + k_q\,(1-\xi)\right]^2}. \tag{A.9}$$

Appendix B. Pure series system

The equivalent stiffness of a system of rods in series is provided by:

$$K_{eq}^{PS} = \left[\frac{1}{k_1} + \frac{1}{k_2} + \cdots + \frac{1}{k_n}\right]^{-1} = \left[\sum_{i=1}^{n}\frac{1}{k_i}\right]^{-1}. \tag{B.1}$$

The total stiffness can be rewritten based on the qth element as:

$$K_{eq}^{PS}(k_q) = \left[\left(\sum_{i=1}^{n}\frac{1}{k_i} - \frac{1}{k_q}\right) + \frac{1}{k_q}\right]^{-1} = \left(\frac{1}{K_{\text{eq},-q}} + \frac{1}{k_q}\right)^{-1} = \left(\frac{k_q + K_{\text{eq},-q}}{k_q K_{\text{eq},-q}}\right)^{-1}, \tag{B.2}$$

where $K_{\text{eq},-q}$ is the equivalent stiffness of the system of rods in series without the contribution of the qth rod. The total work of deformation, considering the linear elasticity, is:

$$W = \frac{1}{2} F\delta = \frac{1}{2}\frac{F^2}{K_{\text{eq}}^{PS}(k_q)} = \frac{1}{2}F^2\frac{k_q + K_{\text{eq},-q}}{k_q K_{\text{eq},-q}}. \tag{B.3}$$

Including the Lemaître and Chaboche formulation proposed in Eq. (A.4) for the stiffness of the qth rod, i.e. $k_{q,\xi}$, the total work of deformation can be rewritten as:

$$W = \frac{F^2}{2}\frac{k_{q,\xi} + K_{\text{eq},-q}}{k_{q,\xi} K_{\text{eq},-q}}. \tag{B.4}$$

The variation of elastic work of deformation due to the variation of the stiffness of $k_{q,\xi}$ is:

$$\frac{\partial W}{\partial k_{q,\xi}} = \frac{F^2}{2}\frac{\left(k_{q,\xi}\ K_{\text{eq},-q}\right) - \left(K_{\text{eq},-q} + k_{q,\xi}\right) K_{\text{eq},-q}}{\left(K_{\text{eq},-q}\ k_{q,\xi}\right)^2}. \tag{B.5}$$

Considering the derivation rule of composite functions reported in Eq. (A.7), the variation of the elastic work with respect to the damage variable is:

$$\frac{\partial W}{\partial \xi} = \frac{F^2}{2}\frac{\left(k_{q,\xi}\ K_{\text{eq},-q}\right) - \left(K_{\text{eq},-q} + K_{q,\xi}\right) K_{\text{eq},-q}}{\left(K_{\text{eq},-q}\ k_{q,\xi}\right)^2} k_q. \tag{B.6}$$

Appendix C. Mixed system

A general expression of the equivalent stiffness of a system of rods in the configuration reported in Fig. 5 is provided by:

$$K_{eq}^{MIX} = \frac{k_1k_3 + k_1k_4 + k_2k_3 + k_2k_4 + k_3k_4}{k_1 + k_2 + k_3}. \tag{C.1}$$

C.1. Damage acting on rod #1

Considering that the stiffness of rod #1 can varies, namely k_1, the equivalent stiffness can be rewritten as:

$$K_{eq}^{MIX}(k_1) = \frac{k_1\left(k_3 + k_4\right) + k_2\left(k_3 + k_4\right) + k_3k_4}{k_1 + k_2 + k_3}. \tag{C.2}$$

The total work of deformation, considering a linear elastic behavior of the system is:

$$W = \frac{1}{2}F\delta = \frac{F^2}{2}\frac{1}{K_{\text{eq}}^{MIX}(k_1)} = \frac{F^2}{2}\left[\frac{k_1\left(k_3 + k_4\right) + k_2\left(k_3 + k_4\right) + k_3k_4}{k_1 + k_2 + k_3}\right]^{-1}. \tag{C.3}$$

Including the Lemaître and Chaboche formulation proposed in Eq. (A.4) for the stiffness of the 1st rod, i.e. $k_{1,\xi}$, the variation of elastic work of deformation due to the variation of the stiffness of the first rod is:

$$\frac{\partial W}{\partial k_{1,\xi}} = -\frac{F^2}{2}\left\{\frac{\left(k_3 + k_4\right)\left(k_{1,\xi} + k_3 + k_4\right)}{\left[k_{1,\xi}\left(k_3 + k_4\right) + k_2\left(k_3 + k_4\right) + k_3k_4\right]^2} + -\frac{1}{k_{1,\xi}\left(k_3 + k_4\right) + k_2\left(k_3 + k_4\right) + k_3k_4}\right\}, \tag{C.4}$$

which can be rewritten as:

$$\frac{\partial W}{\partial k_{1,\xi}} = -\frac{F^2}{2}\left[\frac{-A + BC}{(A + Bk_{1,\xi})^2}\right], \tag{C.5}$$

with $A = k_2k_3 + k_2k_4 + k_3k_4$, $B = k_3 + k_4$, and $C = k_2 + k_3$. The variation of $k_{1,\xi}$ with respect to the damage variable is:

$$\frac{\partial k_{1,\xi}}{\partial \xi} = -k_1. \tag{C.6}$$

Considering the derivation rule of composite functions reported in Eq. (A.7), the variation of the elastic work with respect to the damage

variable is:

$$\frac{\partial W}{\partial \xi} = \frac{F^2}{2}\left[\frac{-A+BC}{(A+Bk_{1,\xi})^2}\right]k_1. \tag{C.7}$$

C.2. Damage acting on rod #2

The damage on rod #2 can be detailed in the same way as per rod #1 (as they are equal). It results that the variation of the elastic work with respect to the damage variable is:

$$\frac{\partial W}{\partial \xi} = \frac{F^2}{2}\left[\frac{-D+BE}{(D+Bk_{2,\xi})^2}\right]k_2, \tag{C.8}$$

with $D = k_1k_3 + k_1k_4 + k_3k_4$, $B = k_3 + k_4$, and $E = k_1 + k_3$.

C.3. Damage acting on rod #3

Considering that the stiffness of rod #3 can varies, namely k_3, the equivalent stiffness can be rewritten as:

$$K_{eq}^{MIX}(k_3) = \frac{k_3(k_1+k_2+k_4)+k_4(k_1+k_2)}{k_1+k_2+k_3}. \tag{C.9}$$

The total work of deformation, considering a linear elastic behavior of the system is:

$$W = \frac{1}{2}F\delta = \frac{F^2}{2}\left[\frac{k_3(k_1+k_2+k_4)+k_4(k_1+k_2)}{k_1+k_2+k_3}\right]^{-1}. \tag{C.10}$$

Including the Lemaître and Chaboche formulation proposed in Eq. (A.4) for the stiffness of the 3rd rod, i.e. $k_{3,\xi}$, the variation of elastic work of deformation due to the variation of the stiffness of the third rod is:

$$\frac{\partial W}{\partial k_{3,\xi}} = -\frac{F^2}{2}\left\{\frac{\left(k_1+k_2+k_{3,\xi}\right)\left(k_1+k_2+k_4\right)}{\left[\left(k_1+k_2\right)\left(k_{3,\xi}+k_4\right)+k_{3,\xi}k_4\right]^2} + -\frac{1}{\left(k_1+k_2\right)\left(k_{3,\xi}+k_4\right)+k_{3,\xi}k_4}\right], \tag{C.11}$$

which can be rewritten as:

$$\frac{\partial W}{\partial k_{3,\xi}} = -\frac{F^2}{2}\left[\frac{G}{GH+(G+H)k_{3,\xi}}\right]^2, \tag{C.12}$$

with $G = k_1 + k_2$, $H = k_4$. The variation of $k_{3,\xi}$ with respect to the damage variable is:

$$\frac{\partial k_{3,\xi}}{\partial \xi} = -k_3. \tag{C.13}$$

Considering the derivation rule of composite functions reported in Eq. (A.7), the variation of the elastic work with respect to the damage variable is:

$$\frac{\partial W}{\partial \xi} = \frac{F^2}{2}\left[\frac{G}{GH+(G+H)k_{3,\xi}}\right]^2 k_3. \tag{C.14}$$

C.4. Damage acting on rod #4

Considering that the stiffness of rod #4 can varies, namely k_4, the equivalent stiffness can be rewritten as:

$$K_{eq}^{MIX}(k_4) = \frac{k_4\left(k_1+k_2+k_3\right)+k_3\left(k_1+k_2\right)}{k_1+k_2+k_3}. \tag{C.15}$$

The total work of deformation, considering a linear elastic behavior of the system is:

$$W = \frac{1}{2}F\delta = \frac{F^2}{2}\left[\frac{k_4\left(k_1+k_2+k_3\right)+k_3\left(k_1+k_2\right)}{k_1+k_2+k_3}\right]^{-1}. \tag{C.16}$$

Including the Lemaître and Chaboche formulation proposed in Eq. (A.4) for the stiffness of the 4th rod, i.e. $k_{4,\xi}$, the variation of elastic work of deformation due to the variation of the stiffness of the fourth rod is:

$$\frac{\partial W}{\partial k_{4,\xi}} = -\frac{F^2}{2}\left[\frac{k_1+k_2+k_3}{k_3k_{4,\xi}+\left(k_1+k_2\right)\left(k_3+k_{4,\xi}\right)}\right]^2, \tag{C.17}$$

which can be rewritten as:

$$\frac{\partial W}{\partial k_{4,\xi}} = -\frac{F^2}{2}\left[\frac{G+J}{GJ+(G+J)k_{4,\xi}}\right]^2, \tag{C.18}$$

with $G = k_1 + k_2$, $J = k_3$. The variation of $k_{3,\xi}$ with respect to the damage variable is:

$$\frac{\partial k_{3,\xi}}{\partial \xi} = -k_3. \tag{C.19}$$

Considering the derivation rule of composite functions reported in Eq. (A.7), the variation of the elastic work with respect to the damage variable is:

$$\frac{\partial W}{\partial \xi} = \frac{F^2}{2}\left[\frac{G+J}{GJ+(G+J)k_{4,\xi}}\right]^2 k_4. \tag{C.20}$$

Data availability

Data will be made available on request.

References

Akyildiz, I.F., Lee, A., Wang, P., Luo, M., Chou, W., 2014. A roadmap for traffic engineering in sdn-openflow networks. Comput. Netw. 71, 1–30.

Bažant, Z.P., Cusatis, G., Cedolin, L., 2004. Temperature effect on concrete creep modeled by microprestress-solidification theory. J. Eng. Mech. 130 (6), 691–699.

Bazant, Z.P., Prasannan, S., 1989. Solidification theory for concrete creep, i: Formulation. J. Eng. Mech. 115 (8), 1691–1703.

Bažant, Z.P., Xiang, Y., Adley, M.D., Prat, P.C., Akers, S.A., 1996. Microplane model for concrete: Ii: data delocalization and verification. J. Eng. Mech. 122 (3), 255–262.

Belluzzi, O., 1946. Scienza Delle Costruzioni, Vol. 1, N. Zanichelli.

Bier, V.M., Nagaraj, A., Abhichandani, V., 2005. Protection of simple series and parallel systems with components of different values. Reliab. Eng. Syst. Saf. 87 (3), 315–323.

Carpinteri, A., 1992. Scienza Delle Costruzioni 1. Società Editrice Esculapio.

Chen, B., 2018. Conceptual design synthesis based on series-parallel functional unit structure. J. Eng. Des. 29 (3), 87–130.

Chen, P.M., Lee, E.K., Gibson, G.A., Katz, R.H., Patterson, D.A., 1994. Raid: High-performance, reliable secondary storage. ACM Comput. Surv. 26 (2), 145–185.

Chopra, A.K., 2007. Dynamics of Structures. Pearson Education India.

Coit, D.W., Smith, A.E., 1996. Reliability optimization of series-parallel systems using a genetic algorithm. IEEE Trans. Reliab. 45 (2), 254–260.

De Biagi, V., 2016. Structural behavior of a metallic truss under progressive damage. Int. J. Solids Struct. 82, 56–64.

De Biagi, V., 2018. Robustness and Complexity of Structures Against Extreme Events (Ph.D. thesis). Politecnico di Torino, Torino, Italy.

De Biagi, V., Chiaia, B., 2013. Complexity and robustness of frame structures. Int. J. Solids Struct. 50 (22–23), 3723–3741.

De Biagi, V., Chiaia, B.M., 2016. Damage tolerance in parallel systems. Int. J. Damage Mech. 25 (7), 1040–1059.

Gere, J.M., Goodno, B.J., 2012. Mechanics of Materials, eigthth ed. Cengage Learning.

Hagen, Ø., Tvedt, L., 1991. Vector process out-crossing as parallel system sensitivity measure. J. Eng. Mech. 117 (10), 2201–2220.

Hohenbichler, M., Rackwitz, R., 1983. Reliability of parallel systems under imposed uniform strain. J. Eng. Mech. 109 (3), 896–907.

Khabbaz, M.J., Assi, C.M., Fawaz, W.F., 2011. Disruption-tolerant networking: A comprehensive survey on recent developments and persisting challenges. IEEE Commun. Surv. Tutor. 14 (2), 607–640.

Kiakojouri, F., De Biagi, V., Abbracciavento, L., 2023. Design for robustness: Bio-inspired perspectives in structural engineering. Biomimetics 8 (1), 95.

Kiakojouri, F., De Biagi, V., Chiaia, B., Sheidaii, M.R., 2020. Progressive collapse of framed building structures: Current knowledge and future prospects. Eng. Struct. 206, 110061.

Knoll, F., Vogel, T., 2009. Design for Robustness, Vol. 11, IABSE.

Lemaitre, J., Chaboche, J.-L., 1994. Mechanics of Solid Materials. Cambridge University Press.

Levitin, G., Lisnianski, A., 2001. A new approach to solving problems of multi-state system reliability optimization. Qual. Reliab. Eng. Int. 17 (2), 93–104.

Lyu, M.R., Rangarajan, S., Van Moorsel, A.P., 2002. Optimal allocation of test resources for software reliability growth modeling in software development. IEEE Trans. Reliab. 51 (2), 183–192.

Mahmood, M.A., Seah, W.K., Welch, I., 2015. Reliability in wireless sensor networks: A survey and challenges ahead. Comput. Netw. 79, 166–187.
Majdzik, P., 2022. A feasible schedule for parallel assembly tasks in flexible manufacturing systems. Int. J. Appl. Math. Comput. Sci. 32 (1).
Manterola, J., 2015. PUENTES Tomo IV (in Spanish). Canales y Puertos Escuela Tecnica Superior de Ingenieros de Caminos, Madrid.
Mughal, A.A., 2018. The art of cybersecurity: Defense in depth strategy for robust protection. Int. J. Intell. Autom. Comput. 1 (1), 1–20.
Nelson, R.B., Dorfmann, A., 1995. Parallel elastoplastic models of inelastic material behavior. J. Eng. Mech. 121 (10), 1089–1097.
Ouiddir, R., Rahli, M., Meziane, R., Zeblah, A., 2004. Ant colony optimization for new redesign problem of multi-state electrical power systems. J. Electr. Eng. Bratislava 55 (3/4), 57–63.
Pathan, R.M., 2017. Real-time scheduling algorithm for safety-critical systems on faulty multicore environments. Real-Time Syst. 53, 45–81.
Pillai, S.B., 2024. Adsorption in water and used water purification. In: Handbook of Water and Used Water Purification. Springer, pp. 99–120.
Prasad, B.R., 2020. Structural Dynamics in Earthquake and Blast Resistant Design. CRC Press.
Roberson, J.A., Cassidy, J.J., Chaudhry, M.H., 1998. Hydraulic Engineering. John Wiley & Sons.
Saxena, S., Sharma, N., Sharma, S., 2013. Image processing tasks using parallel computing in multi core architecture and its applications in medical imaging. Int. J. Adv. Res. Comput. Commun. Eng. 2 (4), 1896–1900.
Shokrollahi, M., Zayeri Baghlan Nejad, A., 2014. Numerical analysis of free longitudinal vibration of nonuniform rods: Discrete singular convolution approach. J. Eng. Mech. 140 (8), 06014007.
Song, J., Der Kiureghian, A., 2003. Bounds on system reliability by linear programming. J. Eng. Mech. 129 (6), 627–636.
Starossek, U., 2009. Progressive Collapse of Structures. Thomas Telford, London.
Starossek, U., Haberland, M., 2011. Approaches to measures of structural robustness. Struct. Infrastruct. Eng. 7 (7–8), 625–631.
Sterbenz, J.P., Hutchison, D., Çetinkaya, E.K., Jabbar, A., Rohrer, J.P., Schöller, M., Smith, P., 2010. Resilience and survivability in communication networks: Strategies, principles, and survey of disciplines. Comput. Netw. 54 (8), 1245–1265.
Taflanidis, A.A., Scruggs, J.T., Beck, J.L., 2008. Reliability-based performance objectives and probabilistic robustness in structural control applications. J. Eng. Mech. 134 (4), 291–301.
Tavakkoli-Moghaddam, R., Safari, J., Sassani, F., 2008. Reliability optimization of series-parallel systems with a choice of redundancy strategies using a genetic algorithm. Reliab. Eng. Syst. Saf. 93 (4), 550–556.
Weng, Y.-H., Qian, K., Fu, F., Fang, Q., 2020. Numerical investigation on load redistribution capacity of flat slab substructures to resist progressive collapse. J. Build. Eng. 29, 101109.
Yalaoui, A., Chu, C., Chatelet, E., 2005. Reliability allocation problem in a series–parallel system. Reliab. Eng. Syst. Saf. 90 (1), 55–61.
Zio, E., 2009. Reliability engineering: Old problems and new challenges. Reliab. Eng. Syst. Saf. 94 (2), 125–141.
Zissis, D., Lekkas, D., 2012. Addressing cloud computing security issues. Future Gener. Comput. Syst. 28 (3), 583–592.